Electronic Supplementary Material (ESI) for Journal of Materials Chemistry B.

Hypoxia-Augmented and Photothermal-Enhanced Ferroptotic Therapy with High Specificity and Efficiency

Peijing An[a], Dihai Gu[a], Zhiguo Gao[a], Fengying Fan[a], Yong Jiang[a], Baiwang Sun[a,*]

a: School of Chemistry and Chemical Engineering, Southeast University, Nanjing 210089, PR China

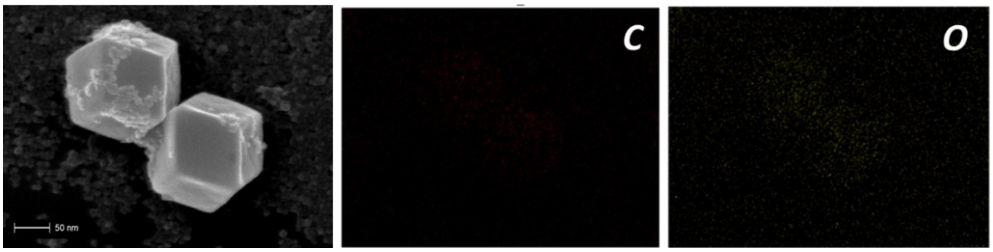

Figure S1. Corresponding elemental mapping of FGGZ.

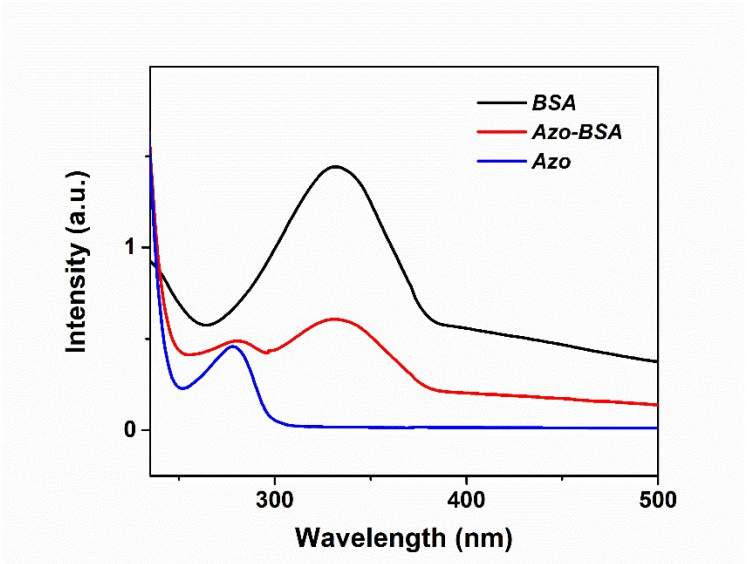

Figure S2. UV/Vis absorption spectra of Azo, BSA and Azo-BSA. Azo exhibited a characteristic absorption peak at 278 nm, and BSA exhibited a characteristic absorption peak at 332 nm. The obvious peaks at 278 nm and 332 nm of Azo-BSA spectrum proved the successful synthesis of Azo-BSA.

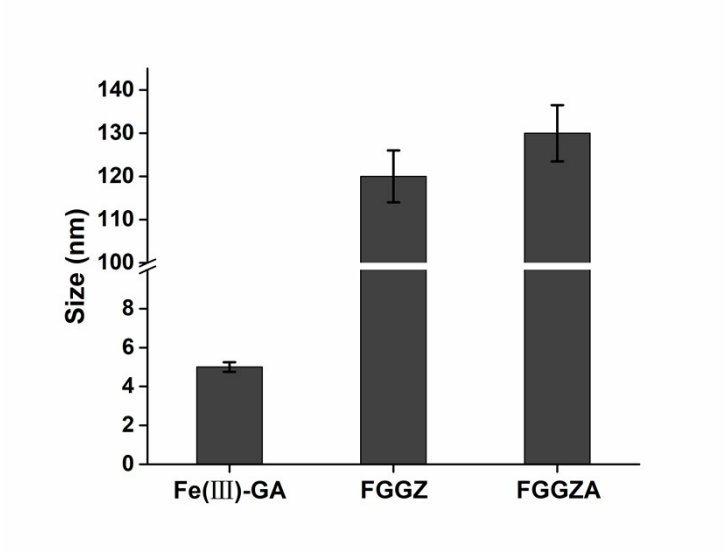

Figure S3. Particle size of Fe(Ⅲ)-GA, FGGZ and FGGZA.

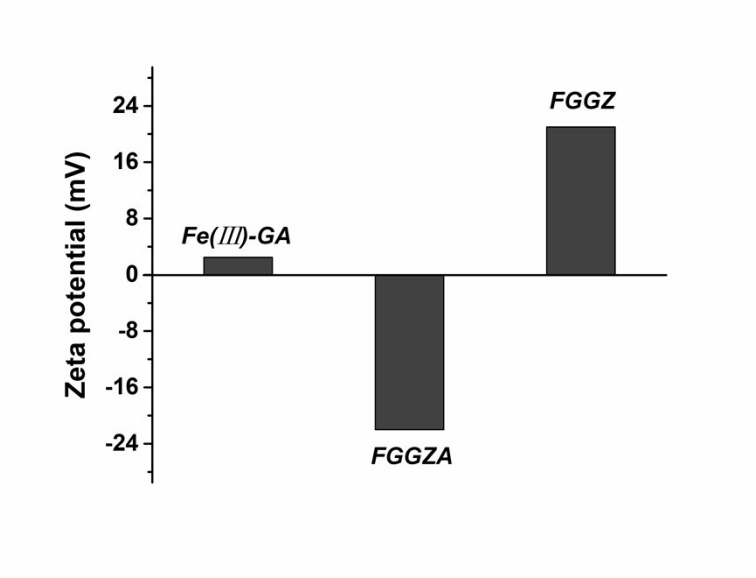

Figure S4. Zeta potential of Fe(Ⅲ)-GA, FGGZ and FGGZA.

The photothermal conversion efficiency (η) was given as:

$$\eta = \frac{hS(T_{max} - T_{surr}) - Q_s}{I(1 - 10^{-A})}$$

$$hS = \frac{\sum m_i C_{p,i}}{\tau s}$$

$$t = \tau s(-\ln \theta)$$

$$\theta = \frac{T - T_{surr}}{T_{max} - T_{surr}}$$

Where m is the mass of sample and equal to 1.0 g, c is the specific heat capacity of water (4.2 J g^{-1}), T_{max} is the maximum temperature and equal to 45.1 ℃, T_{surr} is the temperature of ambient surroundings and equal to 26.1 ℃. The Qs expresses the heat associated with the light absorbance, I is the laser power density and equal to 1.0 W, and A is absorption of Fe(Ⅲ)-GA aqueous solution at 808 nm and equal to 0.8588. The t is cooling time after irradiation. Finally, the photothermal conversion efficiency is calculated to be 66.5%.

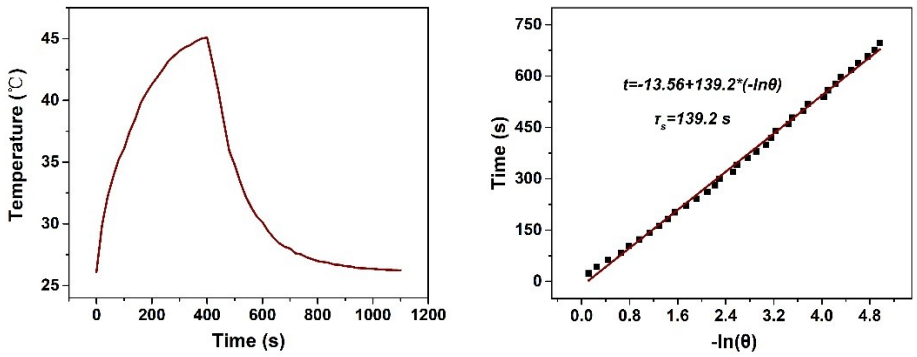

Figure S5. a) Heating and cooling curces of Fe(Ⅲ)-GA aqueous solution (100 μg mL^{-1}) under irradiation of 808 nm laser (1 W cm^{-2}). b) Linear time data versus-lnθ obtained from the cooling period.

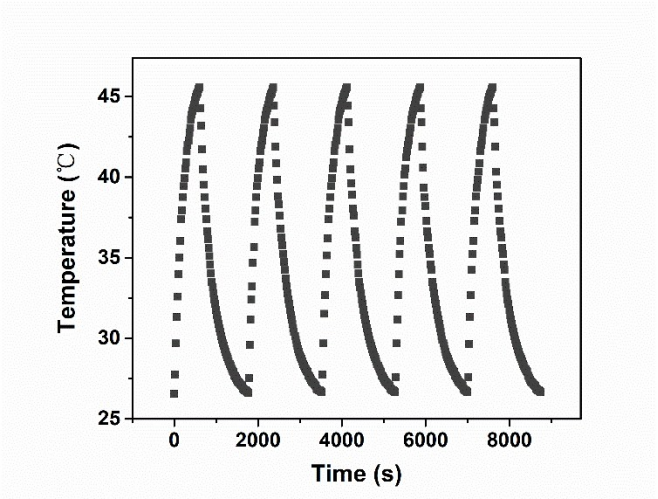

Figure S6. Temperature variations of Fe(Ⅲ)-GA aqueous solution over five laser on/off cycles irradiated by 808 nm laser.

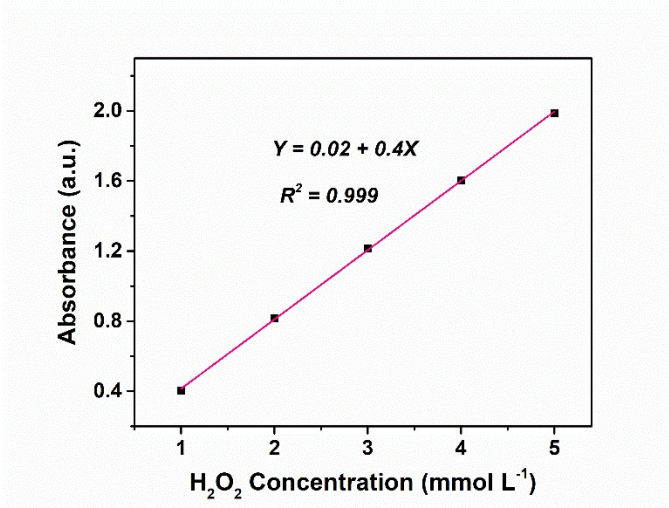

Figure S7. Standard calibration curve of H_2O_2 aqueous solution.

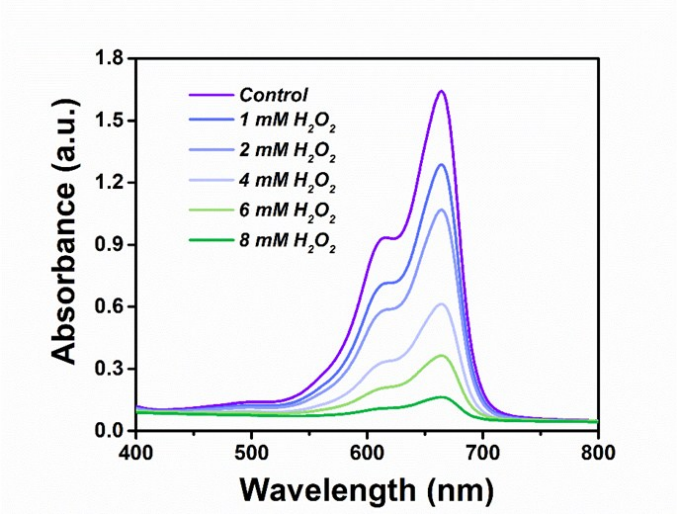

Figure S8. Degradation of MB with different concentration of H_2O_2. The degradation of MB significantly increased with the H_2O_2 concentration increasing.

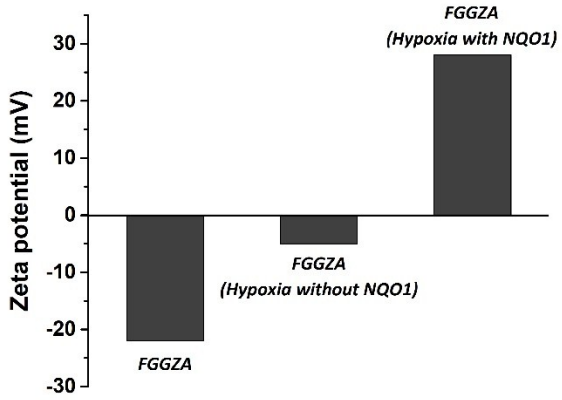

Figure S9. Zeta potential of FGGZA under various conditions.

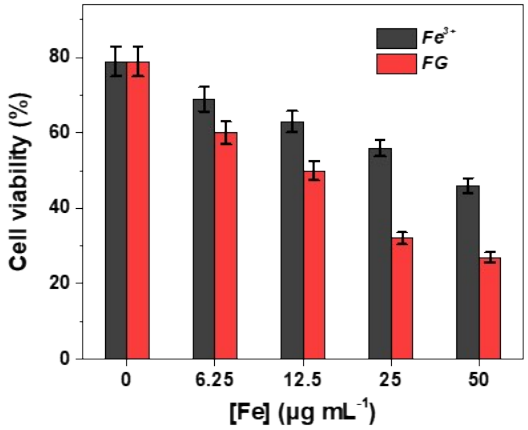

Figure S10. The cell viability of MCF-7 cells after 24 h of incubation of Fe^{3+} and Fe(Ⅲ)-GA.

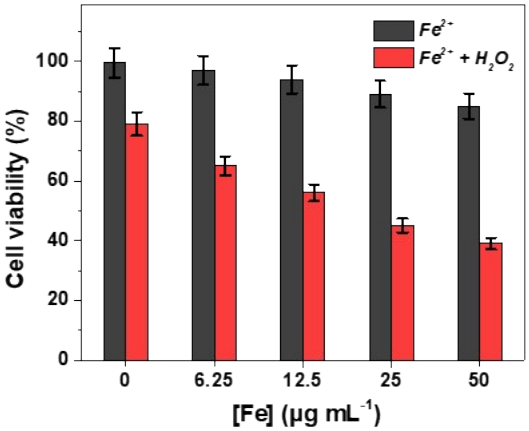

Figure S11. The cell viability of MCF-7 cells after 24 h of incubation of Fe^{2+} plus H2O2 compared with Fe^{2+}.

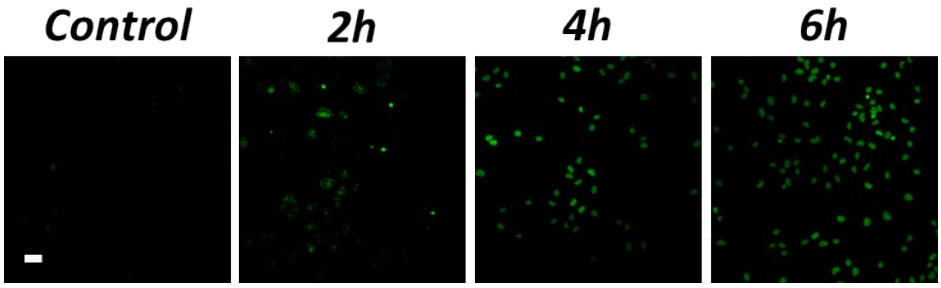

Figure S12. Qualitatively analysis of generated ROS in MCF-7 cells after incubation with Fe^{2+} measured by CLSM. (Scale bar, 40 nm)

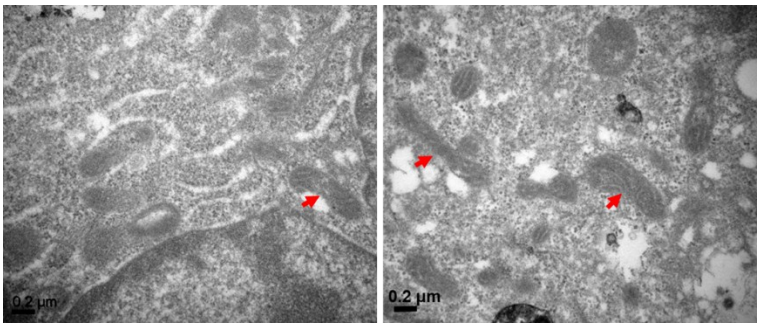

Figure S13. TEM image of MCF-7 cells treated with FGGZA plus NIR showing intact nucleus with complete structure and shrunken mitochondria with dense membrane.

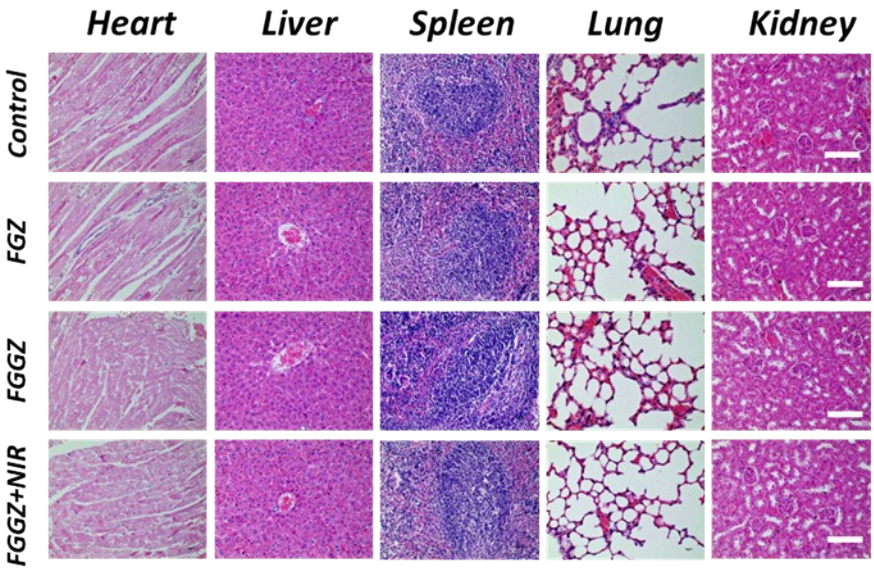

Figure S14. H&E stained images of major organ slices exposed to different groups. (bar = 100 μm).